LBL-13610
Preprint

Lawrence Berkeley Laboratory
UNIVERSITY OF CALIFORNIA

Submitted to Physical Review Letters

A THIRD DISCONTINUITY IN THE YRAST LEVELS OF ^{158}Er

J. Burde, E.L. Dines, S. Shih, R.M. Diamond,
J.E. Draper, K.H. Lindenberger, C. Schück,
and F.S. Stephens

December 1981

NUCLEAR SCIENCE DIVISION

Prepared for the U.S. Department of Energy under Contract W-7405-ENG-48

LBL-13610

A Third Discontinuity in the Yrast Levels of ^{158}Er

J. Burde, E.L. Dines,[†] S. Shih, R.M. Diamond,
J.E. Draper,[†] K.H. Lindenberger, C. Schück, and F.S. Stephens

Nuclear Science Division
Lawrence Berkeley Laboratory
University of California
Berkeley, CA 94720

Abstract

Discrete yrast transitions from states with spins up to I = 38 have been observed in ^{158}Er via the reaction ^{122}Sn(^{40}Ar,4nγ). In addition to the pronounced backbend at I = 14 and the upbend at I = 28 previously known, the start of a third yrast discontinuity at I = 38 is indicated. Candidates for the I = 40 state are suggested and possible causes of the yrast discontinuity are discussed.

This work was supported by the Director, Office of Energy Research, Division of Nuclear Physics of the Office of High Energy and Nuclear Physics of the U.S. Department of Energy under Contract W-7405-ENG-48.

In rare-earth nuclei states with angular momenta up to $I \simeq 70$ can survive particle evaporation following heavy-ion fusion reactions.1) However, the nuclear structure of states of very high angular momentum can be studied only through unresolved de-excitation γ rays.2) Resolved gamma lines from collective states have usually been observed only for $I < 30$, although for non-collective states spins as high as $I = 38$ have been identified.3) Many attempts have been made to extend these angular momentum limits because discrete γ rays can give more detailed nuclear structure information. The discovery4) of "backbending", where the regular frequency increase with spin is temporarily reversed, produced many investigations of collective states by (HI,xn) reactions and by Coulomb excitation. The explanation usually given for this discontinuity in the yrast levels is the alignment of the angular momentum of two high-j nucleons with the rotational angular momentum.5) In ^{158}Er the backbend at $I = 14$ has been attributed to the alignment of a pair of $i_{13/2}$ neutrons,6,7) and the upbend at $I = 28$ has been considered as due most probably to alignment of a pair of $h_{11/2}$ protons.8) The aim of the present investigation was to study still higher members of the yrast sequence.

The high spin yrast levels in ^{158}Er have been produced in the ^{122}Sn(^{40}Ar,4n) reaction using 170 MeV ^{40}Ar from the 88-inch Cyclotron of the Lawrence Berkeley Laboratory. The lifetimes of the states with spins $\geqslant 20\ \hbar$ observed in the present experiment are expected to be comparable to the stopping time of the excited recoiling nuclei in the target. Hence, with a thick target, 1 MeV γ lines will have a width corresponding to the full Doppler shift (2%) of 20 keV. The broadening can be minimized by using a sufficiently thin target and placing the detector in a direction parallel to the beam, where the effect due to the finite acceptance angle is the smallest. To insure narrow lines without unduly reducing the yield, the target consisted of four self-supporting ^{122}Sn foils, 0.5 mg/cm^2 thick, separated from each other by 0.5 mm (ample for most of the states to decay in flight).

To enhance the coincidence counting rate in order to see the weak high-spin transitions, five Ge(Li) coaxial detectors were used. Four of them (of 20, 20, 15, and 10% efficiency) were placed at the most backward angles available, ±(155° to 160°) with respect to the beam. The fifth detector (10%) was placed alternatively at 0° or 90° for an angular distribution determination. All these detectors were about 10 cm from the target. A multiplicity filter consisting of five 7.6 x 7.6 cm NaI detectors surrounded the target, and the number of NaI detectors firing in coincidence with each event (fold) was recorded. Each event consisted of a γ-γ coincidence between two of the five Ge(Li) detectors, gated by one or more detectors in the multiplicity filter. About 10^8 events were recorded and subsequently analyzed by placing gates on the Ge(Li) energy, the Ge(Li)-NaI TAC, and the fold spectra.

The upper part of figure 1 shows the sum of the $\geqslant$1-fold γ-γ coincidence spectra observed by the four backward Ge(Li) detectors gated by the sum of transitions that de-excite the 18^+ to 32^+ levels (after background subtraction). Below this are similar spectra gated by the three well-defined highest energy lines. It is clear that these three peaks, labeled $34^+ \rightarrow 32^+$, $36^+ \rightarrow 34^+$, and $38^+ \rightarrow 36^+$, are in coincidence with the main sequence of the yrast band. The yields of the γ-ray transitions (Ge(Li) singles) were measured at 0° and 90° for fold $\geqslant$3, and the ratio of these is given in Table 1. These anisotropies are consistent with stretched E2 decays ($\sim$1.4). From the data in Table 1 the yrast level sequence can be established with reasonable certainty up to $I = 38$.

In addition to the well-defined peaks, there are weaker lines from: (1) other product nuclei, (2) side band transitions in ^{158}Er, and (3) higher members of the yrast band. In an attempt to find any higher members, 15 weak lines in the region of 900 to 1300 keV were considered as possible candidates. The data were resorted in coincidence with these 15 lines. In two cases it appeared from the resulting spectra that the lines feed the whole sequence of the yrast band. To make this more quantitative, the intensity of each yrast line from these spectra (after background subtraction) was divided by the intensity of the same line obtained from the sum of gates on the transitions from the 34^+, 36^+, and 38^+ states. Examples of such ratios are given in Table 2. The weighted averages of the transitions indicated in the third and fourth columns have been normalized to those from the 6^+ to 24^+ levels. If a line feeds the whole sequence from above the 38^+ state, the ratios should be constant (unity) up to the transition from the 32^+ state and exceed one for the three higher energy lines due to the suppression of their intensity in the summed spectrum used for the denominator. As can be seen, cases a and b comply with this requirement, whereas the remaining three, chosen as typical for all the other lines examined, do not. This result was found to be insensitive to reasonable changes in the background subtractions. The line at 1067 keV (case a) appears in Fig. 1 weakly, but as a distinct shoulder just above the $38^+ \rightarrow 36^+$ transition, and we tentatively consider it as the most likely $40^+ \rightarrow 38^+$ member of the yrast band. The other line at 1155 keV (case b) might be another 40^+ state that belongs to the previous yrast band. These 40^+ assignments, however, are quite tentative.

Figure 2 shows a plot of the moment of inertia versus the rotational frequency. The beginning of a discontinuity at the 38^+ state can be seen. This discontinuity would be continued by the tentative 40^+ member. From these data one can construct a plot of I vs $\hbar\omega$ (center of Fig. 2) according to the prescription given in ref. 9. At the bottom of Fig. 2, the relative aligned angular momentum, i, is shown. For the first two discontinuities we find ($\hbar\omega$, Δi) to be (0.28, 10) and (0.43, 6), respectively. The first of these sets is in agreement with the previous determinations for ^{158}Er and the second is similar to that found for ^{160}Yb (ref. 10). They support the previous suggestions that $i_{13/2}$ neutrons and $h_{11/2}$ protons, respectively, are the particles responsible for the effects.[6,8]

It is interesting to consider the origin of the third discontinuity indicated at $\hbar\omega \sim 0.53$ MeV. It seems most likely to be the alignment with the rotation axis of an additional high-j particle pair, thus continuing the trend for the nucleus to share its angular momentum between the collective rotation and the alignment of high-j particles. At the first backbend two $i_{13/2}$ neutrons contribute $\sim$10 $\hbar$ of aligned angular momentum to a total spin of 16 $\hbar$. At the second discontinuity (an upbend), the pair of $h_{11/2}$ protons adds another 6 $\hbar$ of aligned angular momentum out of a total spin of 28 $\hbar$. Although the angular momentum alignment is not yet determined, it seems most likely that the third discontinuity is due to either $h_{9/2}$ neutrons or $h_{9/2}$ protons. Of these, the calculations[11,12] for $h_{9/2}$ neutrons give closer agreement with the experimental $\hbar\omega$.

The present work indicates a third discontinuity in yrast levels at about spin 40 $\hbar$ in ^{158}Er. This has been observed by (1) using ^{40}Ar projectiles to bring in high angular momenta, (2) minimizing the Doppler broadening without compromising the coincidence counting rate by employing a target of four thin foils and using four Ge(Li) detectors at backward angles, and (3) enhancement of a particular reaction channel with a γ-ray multiplicity filter. The discontinuity is probably due to alignment of a third pair of particles, most likely $h_{9/2}$ neutrons.

This work was supported by the Director, Office of Energy Research, Division of Nuclear Physics of the Office of High Energy and Nuclear Physics of the U.S. Department of Energy under Contract W-7405-ENG-48.

References

†Department of Physics, University of California, Davis, CA 95616.

1. J.O. Newton, I.Y. Lee, R.S. Simon, M.M. Aleonard, Y. El-Masri, F.S. Stephens, and R.M. Diamond, Phys. Rev. Lett. 38, 810 (1977)
2. R.S. Simon, M.V. Banaschik, P. Colombani, D.P. Soroka, F.S. Stephens, and R.M. Diamond, Phys. Rev. Lett. 36, 359 (1976)
3. T.L. Khoo, R.K. Smither, B. Haas, O. Häusser, H.R. Andrews, D. Horn, and D. Ward, Phys. Rev. Lett. 41, 1027 (1978)
4. A. Johnson, H. Ryde, and J. Sztarkier, Phys. Lett. 34B, 605 (1971)
5. F.S. Stephens, Rev. Mod. Phys. 47, 43 (1975)
6. E. Grosse, F.S. Stephens, and R.M. Diamond, Phys. Rev. Lett. 31, 840 (1973) and 32, 74 (1974)
7. I.Y. Lee, M.M. Aleonard, M.A. Deleplanque, Y. El-Masri, J.O. Newton, R.S. Simon, R.M. Diamond, and F.S. Stephens, Phys. Rev. Lett. 38, 1454 (1977)
8. A. Faessler and M. Plaszajczak, Phys. Lett. 76B, 1 (1978)
9. R. Bengtsson and S. Frauendorf, Nucl. Phys. A327, 139 (1979)
10. L.L. Riedinger, Phys. Scripta 24, 312 (1981)
11. M. Ploszajczak and A. Faessler, Z. Physik A283, 349 (1977)
12. S. Frauendorf, Phys. Scripta 24, 349 (1981)

Table 1

Gamma-Ray Energies, Relative Intensities and Anisotropies

$I_i \rightarrow I_f$	E_γ(keV)	Rel.Intens.*	I(0°)/I(90°)
$6^+ \rightarrow 4^+$	443.4 (3)	100	1.13 (6)
$8^+ \rightarrow 6^+$	523.7 (3)	98 (5)	1.60 (7)
$10^+ \rightarrow 8^+$	579.8 (3)	64 (3)	1.46 (7)
$12^+ \rightarrow 10^+$	608.8 (3)	48 (3)	1.45 (7)
$14^+ \rightarrow 12^+$	510.4 (6)	47 (3)**	**
$16^+ \rightarrow 14^+$	473.3 (3)	54 (3)	1.75 (8)
$18^+ \rightarrow 16^+$	566.9 (3)	39 (2)	1.54 (8)
$20^+ \rightarrow 18^+$	659.4 (4)	23 (1)	1.29 (8)
$22^+ \rightarrow 20^+$	740.0 (4)	17 (1)	1.41 (8)
$24^+ \rightarrow 22^+$	806.2 (4)	11 (1)	1.39 (8)
$26^+ \rightarrow 24^+$	846.0 (6)	5.1 (8)	1.17 (10)
$28^+ \rightarrow 26^+$	859.2 (6)	4.1 (8)	1.51 (15)
$30^+ \rightarrow 28^+$	876.5 (7)	3.1 (5)	2.00 (35)
$32^+ \rightarrow 30^+$	906.7 (7)	1.9 (5)	1.26 (35)
$34^+ \rightarrow 32^+$	960.3 (10)	1.7 (5)	1.26 (35)
$36^+ \rightarrow 34^+$	1018.7 (15)	0.9 (5)	1.91 (40)
$38^+ \rightarrow 36^+$	1061.3 (15)	0.6 (3)	--
a	1067.0 (15)	0.2 (1)	--
b	1156.0 (20)	0.1 (1)	--

*For transitions from states with $I \geq 26\,\hbar$, summed coincidence spectra with gates on 18^+ through 24^+ were used.

**May contain a contribution from annihilation radiation.

Table 2

Evaluation of 40^+ Candidates

40^+ Candidates (keV)	6^+-24^+	26^+-32^+	34^+-38^+
1033	(1.00)	0.60 (11)	0.76 (18)
1067 (a)	(1.00)	0.96 (10)	1.17 (15)
1080	(1.00)	0.95 (11)	0.70 (16)
1091	(1.00)	1.06 (17)	0.51 (28)
1156 (b)	(1.00)	1.09 (14)	1.37 (21)

Figure Captions

Fig. 1. Coincident γ-ray spectra from the reaction $^{122}Sn(^{40}Ar,4n)^{158}Er$ obtained with indicated gates.

Fig. 2. Plots of the moment of inertia (top), yrast spin (middle), and spin alignment (bottom) vs the rotational frequency.

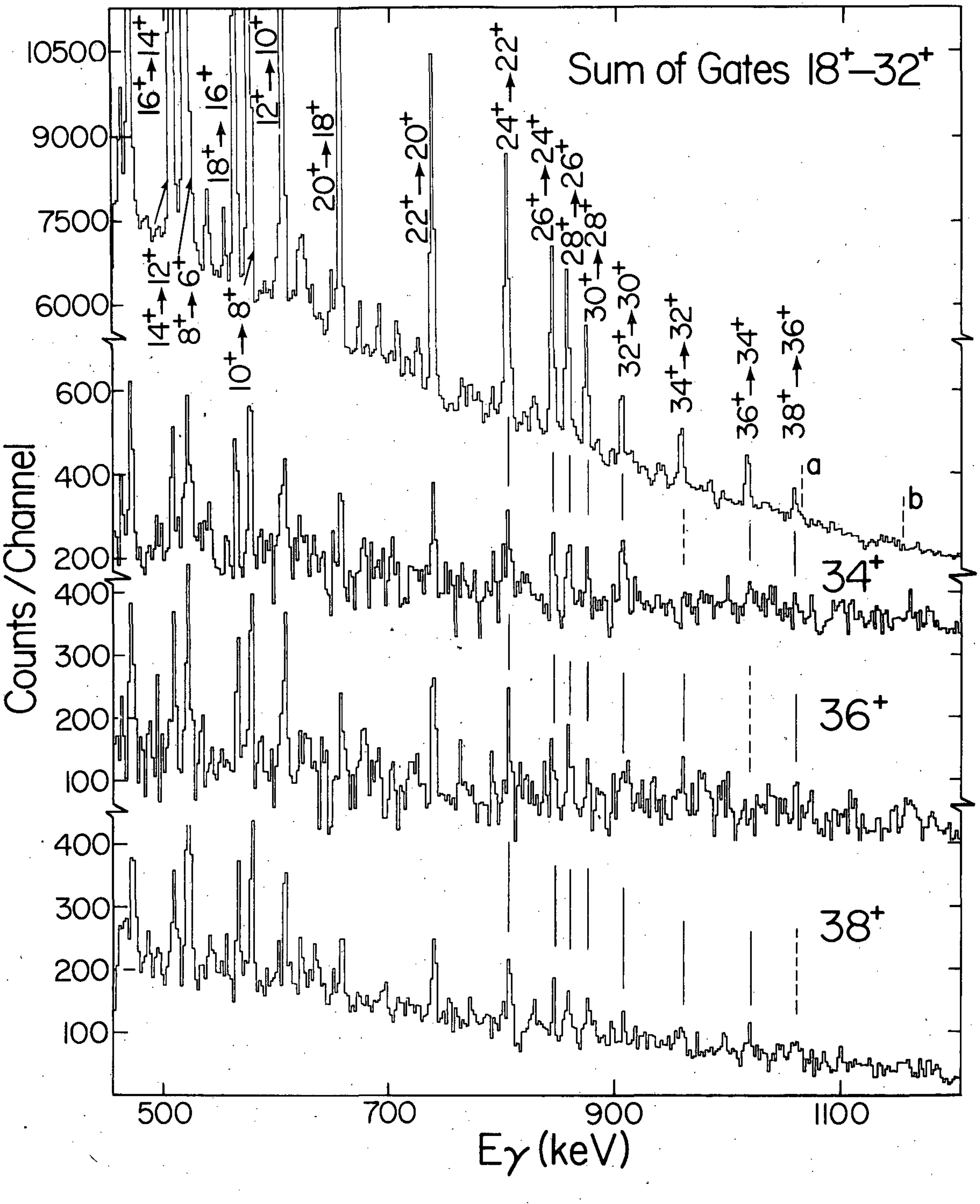

XBL 8111-1577

Fig. 1

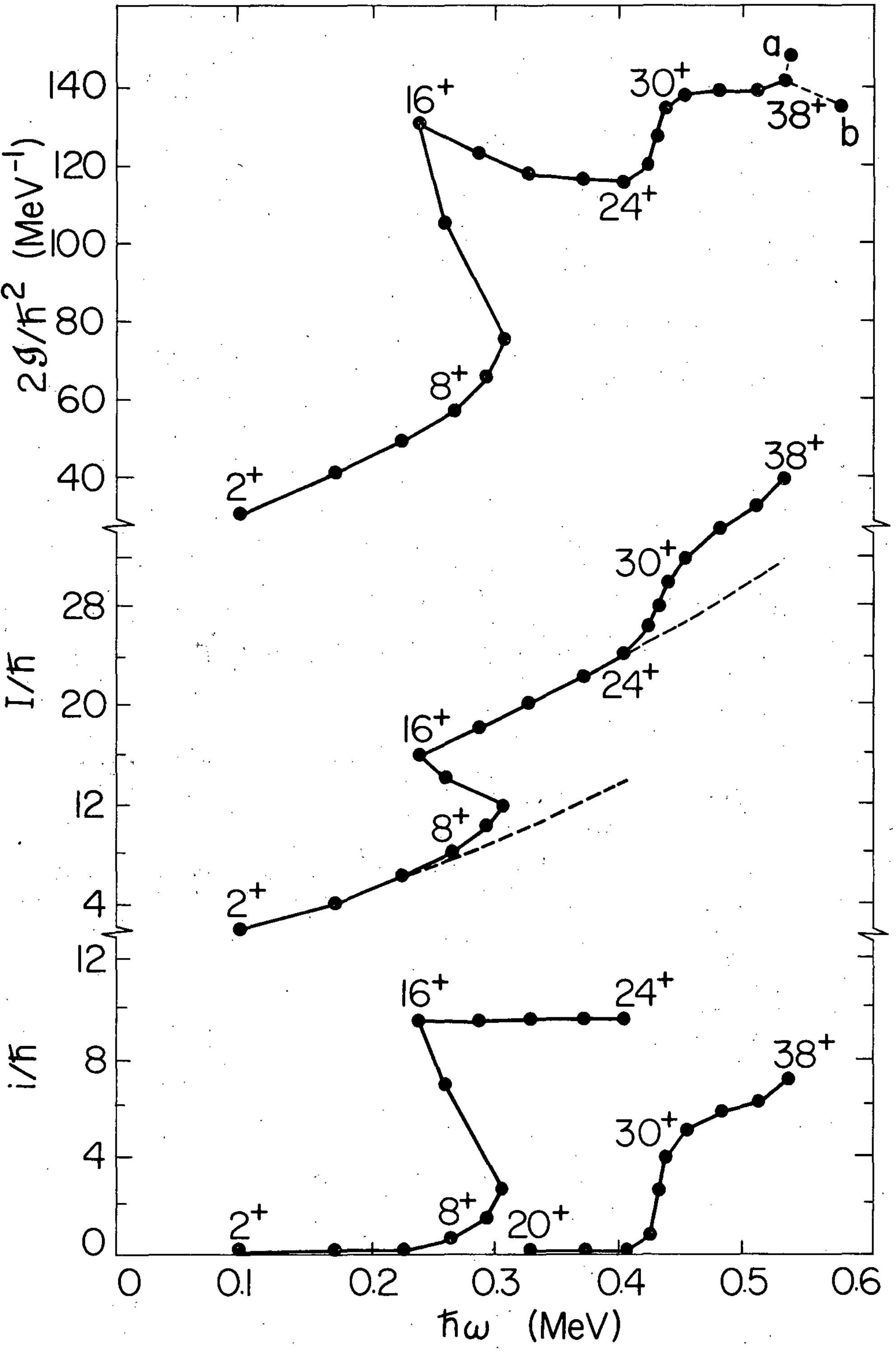

XBL 8111-1576

Fig. 2

TECHNICAL INFORMATION DEPARTMENT
LAWRENCE BERKELEY LABORATORY
UNIVERSITY OF CALIFORNIA
BERKELEY, CALIFORNIA 94720